

## Energies and widths of triply excited $n = 2$ intrashell autoionizing states of $\text{He}^-$

Mirosław Bylicki<sup>1</sup> and Cleanthes A. Nicolaides<sup>2</sup>

<sup>1</sup>*Instytut Fizyki, Uniwersytet Mikołaja Kopernika, Grudziądzka 5, 87-100 Toruń, Poland*

<sup>2</sup>*Theoretical and Physical Chemistry Institute, National Hellenic Research Foundation, 48 Vasileos Constantinou Avenue, 11635 Athens, Greece*

(Received 9 August 1994)

We have computed to high accuracy the energies and the total widths of five triply excited  $n = 2$  intrashell resonances in  $\text{He}^-$ , the  $2s^2 2p^2 P^o$ ,  $2s 2p^2 D^e$ ,  $4P^e$ ,  $2P^e$ , and  $2p^3 D^o$ . These states are characterized by strong localized and asymptotic correlation effects and by their proximity to He doubly excited states. The possible many open channels correspond not only to one- but also to two-electron continua. The resonance parameters were established by applying the complex-coordinate rotation method with large basis sets of orbital and  $r_{ij}$ -correlated configurations. The expansion length of the trial wave functions went up to 1300 terms for the  $2s 2p^2 D^e$  resonance. This resonance is found to be below the He  $2s 2p^3 P^o$  threshold, in agreement with experimental observations and contrary to existing theoretical results. Similarly, the position of the  $2s 2p^2 P^e$  resonance is also below the He  $2p^2 P^e$  threshold, in agreement with a recent theoretical prediction. The widths of these states range from 10 meV for the  $2s 2p^2 P^e$  to 331 meV for  $2p^3 D^o$ .

PACS number(s): 31.50.+w, 32.80.Dz

### I. INTRODUCTION

The  $\text{He}^-$  states arising from the  $n = 2$  intrashell configurations  $2s^2 2p$ ,  $2s 2p^2$ , and  $2p^3$  correspond to resonances in the continuous spectrum of He [1], with the exception of  $2p^3 S^o$ , which localized electron correlation pushes below the He  $2p^2 P^e$  bound state [2] and symmetry does not allow its radiationless decay via Coulomb autoionization [3].

In spite of numerous experimental and theoretical studies of these prototypical states [1–28], for some of them definitive information about accurate decay widths or about energy positions relative to thresholds of doubly excited states (DES's) of He is still lacking. Related issues were brought forth in recent theoretical analyses and computational studies of these states [26,27], such as the question of the identity and position of the  $\text{He}^-$  resonance structure of  $2D$  symmetry relative to the He  $2s 2p^3 P^o$  threshold at 58.31 eV and the question of the rigorous and reliable calculation of its autoionization width. We note that for the  $2s 2p^2 D^e$  as well as the  $2s^2 2p^2 P^o$  state, the available theoretical widths from the early close-coupling calculations of Smith *et al.* [14] do not agree with the experimental ones. On the other hand, the  $2s 2p^2 P^e$ ,  $2p^3 D^o$ , and  $2p^3 P^o$  resonances have not yet been identified experimentally.

In this paper we present results of accurate calculations of the positions and the widths of the  $\text{He}^- n = 2$  intrashell resonances. The main problems which appear when one aims at the calculation of the properties of such states are the following. (1) The applied theory must formally allow the calculation of interelectronic interactions representing localized as well as asymptotic correlations, where the continuum contains one- as well as two-electron interacting open channels. In the recent treatment of these resonances [27], the two-electron continua

were neglected and the widths were calculated in the independent-channel approximation (ICA). (2) The extreme proximity to thresholds of DES's of He requires very high accuracy in the calculation of wave functions and energies, since the relative position of the negative-ion resonances to these thresholds determines whether a particular channel is open or closed. (3) For such states, the calculation of the autoionization widths is more sensitive than usually to the details of the wave functions. The function space used for the application of the theory must contain accurate representations of the localized one-, two-, and three-electron correlations, as well as the scattering orbitals, of their interchannel coupling, and of their interaction with the core. Since the He DES's are highly polarizable [29], this last interaction, which was neglected in [27], may affect the width.

Given these requirements and our experience with the calculation of resonances, we decided to tackle this problem by using the complex-coordinate rotation (CCR) method [30–32], in conjunction with large basis sets having explicit  $r_{ij}$  dependence. The construction of the correlated trial wave functions was carried out as in previous CCR calculations on resonances of three-electron atoms [28,33], using the techniques developed by Woźnicki and co-workers [34,35] for discrete states and real Hamiltonians. The method is briefly reviewed in Sec. II. The results are presented and discussed in Sec. III.

### II. METHOD OF COMPUTATION

The total wave functions  $\Psi$  are chosen to have the form

$$\Psi = \sum_R c_R \Phi_R, \quad (2.1)$$

where the  $\Phi_R$  are products of orbital configuration and

functions of  $r_{ij}$  [34–36]. Basis sets with  $r_{ij}$  factors are known to speed up convergence in ground states such as  $1s^2$  or  $1s^2 2s$ . On the other hand, the structure of highly excited states is different, due to the importance of the multiconfigurational self-consistent field, to large electron radii, and to heavy mixing among different configurations. These facts require the use of at least appropriate orbital configurations for reasonable accuracy to be reached [27,37]. Thus, in this and in our previous work [28], by using very large expansions in (1), we expect that all the crucial orbital, configuration-interaction (CI), and  $r_{ij}$ -dependent details of the Hilbert space contributing to the complex eigenvalues of these three-electron resonances are taken into account.

In the case of an  $LS$ -coupled state, the correlated configurational function of the total quantum numbers  $L, M, S$ , and  $M_S$  can be written as

$$\Phi_R = \hat{A} [ {}^{LM}F_K(\mathbf{r}_1, \dots, \mathbf{r}_N) r_{ij}^\nu \chi_{SM_S} ], \quad (2.2)$$

where  $\hat{A}$  is the  $N$ -electron antisymmetrizer,  ${}^{LM}F_K$  is a spatial function corresponding to the configuration  $K$ ,  $\chi_{SM_S}$  is an  $N$ -electron spin function, and  $r_{ij}^\nu$  is a non-negative power  $\nu$  of the interelectronic distance  $r_{ij}$ . The spatial function  ${}^{LM}F_K$  is, due to the angular symmetry requirements, a linear combination of the products of Slater-type orbitals corresponding to the configuration  $K$ . For  $\nu=0$  the correlation factor becomes equal to 1 and  $\Phi_R$  becomes the usual configurational function. In an actual calculation both  $\nu=0$  and  $\nu \neq 0$  terms should be present.

The basis set described above is nonorthogonal, i.e., the overlap matrix  $\mathbf{S}$  is a nondiagonal matrix. In order to simplify the calculations, the  $\mathbf{T}$  and  $\mathbf{V}$  matrices, representing, respectively, the kinetic and the potential parts of the original (unrotated) Hamiltonian, were calculated in this basis set and were then transformed to an

orthonormal basis set by symmetric orthogonalization:

$$\mathbf{T}' = \mathbf{S}^{-1/2} \mathbf{T} \mathbf{S}^{-1/2}, \quad \mathbf{V}' = \mathbf{S}^{-1/2} \mathbf{V} \mathbf{S}^{-1/2}. \quad (2.3)$$

Once the transformed matrices  $\mathbf{T}'$  and  $\mathbf{V}'$  were computed, they were used to diagonalize the rotated Hamiltonian matrix

$$\mathbf{H}(\theta) = \mathbf{T}' e^{-2i\theta} + \mathbf{V}' e^{-i\theta} \quad (2.4)$$

for as many values of the complex rotation angle  $\theta$  as necessary for finding the optimum energy.

In order to select the proper eigenvalue of  $\mathbf{H}(\theta)$ , corresponding to a given resonance, the well-known procedure was followed [31,32]. The complex eigenvalues computed in a given basis for several values of  $\theta$  form  $\theta$  trajectories on the complex plane. When the quantity  $|dE/d\theta|$  goes through a local minimum versus  $\theta$ , the corresponding complex energy  $E$  characterizes the sought-after resonance.

### III. RESULTS AND DISCUSSIONS

We performed CCR computations for  $\text{He}^-$  for all the  $n=2$  intrashell resonances that can be derived from the  $2s^2 2p$ ,  $2s 2p^2$ , and  $2p^3$  configurations. Stabilized results were obtained for the  $2s^2 2p^2 P^o$ ,  $2s 2p^2 D^e$ ,  $2s 2p^2 P^e$ ,  $2s 2p^2 P^e$ , and  $2p^3 D^o$  states. The basis sets used for them are summarized in Table I. The angular types of three-electron configurations,  $l_1 l_2 l_3$ , are listed together with corresponding numbers of radial terms: the number of orbital configurations,  $K$ , and the number of  $r_{ij}$ -correlated configurations,  $K_r$ . The basis used for the representation of  $2s 2p^2 P^e$  is the smallest. This is mainly because the quartet symmetry allows only one way of spin coupling, in contrast to doublet states, where two ways of spin coupling are possible. Another reason is the number of open channels which have to be properly

TABLE I. Basis sets for the CCR calculation of the triply excited  $\text{He}^-$  resonances. Each angular type of configuration  $l_1 l_2 l_3$ , was represented by  $K$  configuration functions constructed of Slater-type orbitals [ $\nu=0$  in Eq. (2)] and  $K_r$  configuration functions of this type multiplied by  $r_{ij}^\nu$  factors ( $\nu=1$  was used in most of these terms; only a few terms with  $\nu=2$  were taken).

Angular type	$2s^2 2p^2 P^o$		$2p^3 D^o$		$2s 2p^2 D^e$		$2s 2p^2 P^e$		$2s 2p^2 P^e$	
	$K$	$K_r$	$K$	$K_r$	$K$	$K_r$	$K$	$K_r$	$K$	$K_r$
<i>ssp</i>	216	416								
<i>spd</i>	96	96	252	104						
<i>ppp</i>	50	50	192	96						
<i>ppf</i>	36	36								
<i>ddp</i>				180						
<i>ddf</i>				176						
<i>spp</i>					250	250	147	124	450	220
<i>ssd</i>					207	90				
<i>spf</i>					132	44				
<i>sdd</i>					84	60	27	24	100	80
<i>fff</i>									60	
<i>ppd</i>					110	70	35	15	156	36
Total	398	598	800	200	783	514	209	163	766	316
		996		1000		1297		372		1082

represented by the basic set. For each of the states under consideration there is an infinity of channels open for its decay. However, because of basis electronic structure features, only a few of them are important. The  $2s2p^2^4P^e$  resonance decays mostly into the  $1s2p(^3P)\epsilon p$  channel. On the other hand, non-negligible contributions to the decay of the  $2s2p^2^2D^e$  state may come from seven single-electron open channels:  $1s2s(^1,3S)\epsilon d$ ,  $1s2p(^1,3P)\epsilon p$ ,  $1s2p(^1,3P)\epsilon f$ , and  $2s^2\epsilon d$ . In addition to configurations and their correlation terms representing these channels, many more configurations must be included in the basis so as to account for localized correlation as well as for two-electron continua.

The  $\theta$  trajectories corresponding to the  $2s^22p^2P^o$ ,  $2s2p^2^2D^e$ ,  $2s2p^2^4P^e$ ,  $2s2p^2^2P^e$ , and  $2p^3^2D^o$  states are shown in Figs. 1–5, respectively. In the figure captions, the reader can find the information on the number of  $\theta$  values used to plot a given  $\theta$  trajectory, and on the optimized energy. One should notice that the sequential points displayed on the  $\theta$  trajectories correspond to the same step of the  $\theta$  variation,  $\Delta\theta=0.04$ . However, the scale in different figures is different. This is because the stabilization property of the  $\theta$  trajectory changes a lot from one case to another.

The best stabilization and accuracy was achieved for the  $2s2p^2^4P^e$  state. This resonance is narrow and quite well separated from the He thresholds. The closest one, the  $2s2p^3P^o$  level, lies about 0.9 eV above the  $2s2p^2^4P^e$  level. The worst stabilization we obtained was for the  $2p^3^2D^o$  state, which is the widest one. In general, the narrower the resonance and the better separated from the thresholds, the better stabilization and accuracy can be reached in a basis of reasonable size. Using basis sets of about 1300 functions we could not obtain the complex

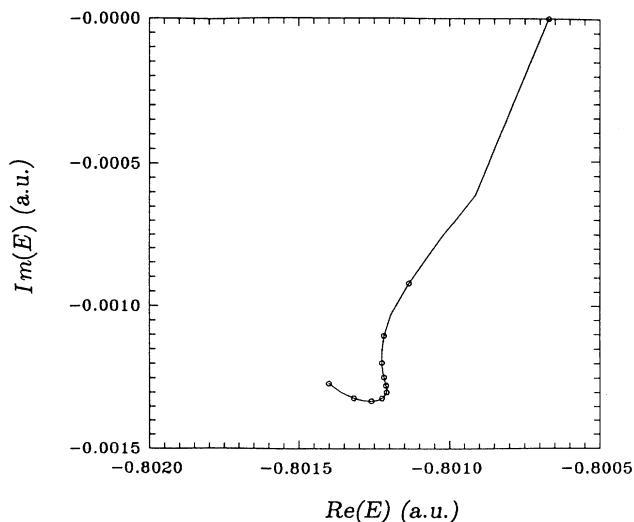


FIG. 1.  $\theta$  trajectory for the  $2s^22p^2P^o$  resonance of  $\text{He}^-$ . The trajectory consists of 22 points, but only the points separated by  $\Delta\theta=0.04$  are displayed. The point on the real axis corresponds to  $\theta=0$  and the last one on the trajectory to  $\theta=0.4$ . The optimum complex energy is  $E = -0.80121 - i \times 0.00130$  a.u., chosen at  $\theta=0.24$ .

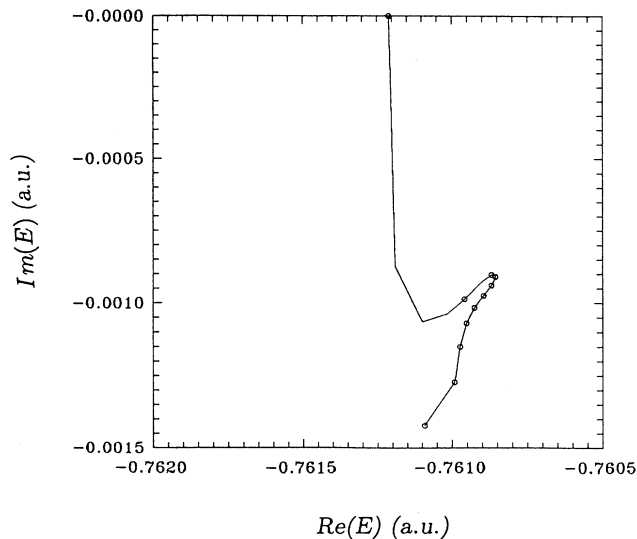


FIG. 2.  $\theta$  trajectory for the  $2s2p^2^2D^e$  resonance of  $\text{He}^-$ . The trajectory consists of 19 points, but only the points separated by  $\Delta\theta=0.04$  are displayed. The point on the real axis corresponds to  $\theta=0$  and the last one on the trajectory to  $\theta=0.4$ . The optimum complex energy is  $E = -0.76086 - i \times 0.00091$  a.u., chosen at  $\theta=0.12$ .

energies for the  $2s2p^2^2S^e$ , and  $2p^3^2P^o$  states stable enough against variation of the complex-rotation angle  $\theta$ . Evidently, their calculation according to the CCR method requires either more carefully optimized or larger basis sets.

The energies and widths of the resonances are given in Table II. The doubly excited two-electron states are also

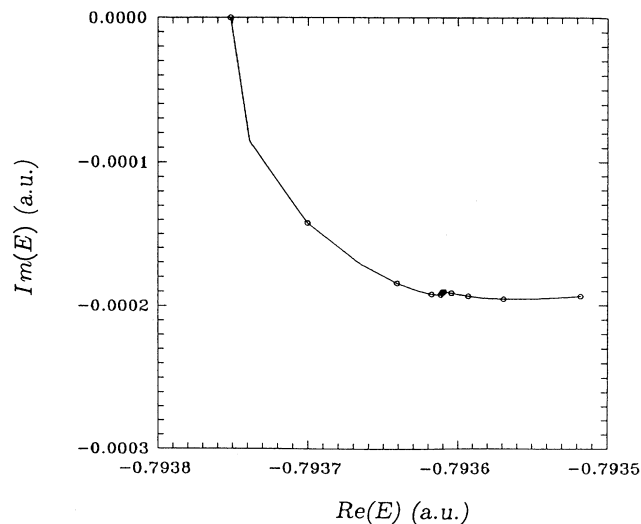


FIG. 3.  $\theta$  trajectory for the  $2s2p^2^4P^e$  resonance of  $\text{He}^-$ . The trajectory consists of 23 points, but only the points separated by  $\Delta\theta=0.44$  are displayed. The point on the real axis corresponds to  $\theta=0$  and the last one on the trajectory to  $\theta=0.44$ . The optimum complex energy is  $E = -0.793610 - i \times 0.000190$  a.u., chosen at  $\theta=0.22$ .

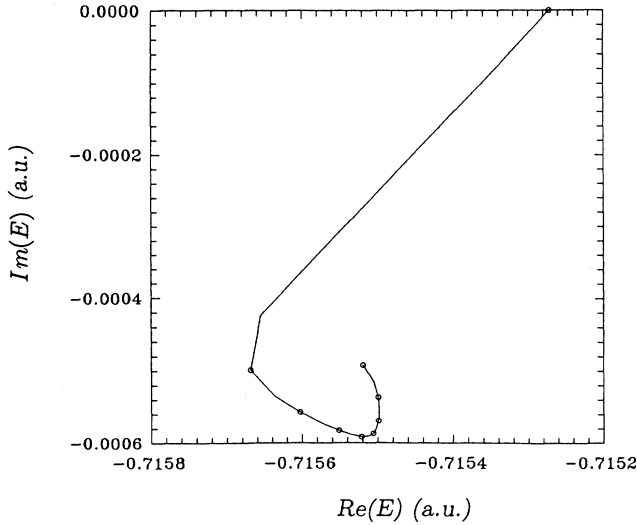


FIG. 4.  $\theta$  trajectory for the  $2s2p^2P^e$  resonance of  $\text{He}^-$ . The trajectory consists of 17 points, but only the points separated by  $\Delta\theta=0.04$  are displayed. The point on the real axis corresponds to  $\theta=0$  and the last one on the trajectory to  $\theta=0.32$ . The optimum complex energy is  $E = -0.71551 - i \times 0.00059$  a.u., chosen at  $\theta=0.18$ .

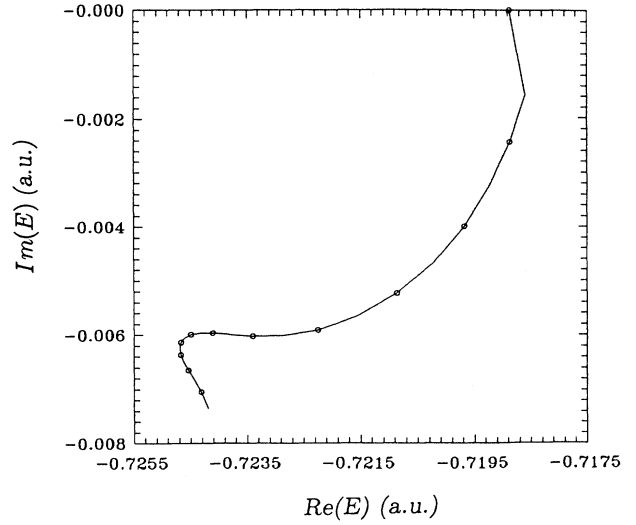


FIG. 5.  $\theta$  trajectory for the  $2p^3D^o$  resonances of  $\text{He}^-$ . The trajectory consists of 24 points, but only the points separated by  $\Delta\theta=0.04$  are displayed. The point on the real axis corresponds to  $\theta=0$  and the last one on the trajectory to  $\theta=0.44$ . The optimum complex energy is  $E = -0.72464 - i \times 0.00609$  a.u., chosen at  $\theta=0.32$ .

given for comparison. The results are compared with a few published theoretical data for the  $2s2p^2P^e$ ,  $2p^3D^o$ , and  $2s2p^2P^e$  states. The position obtained for the  $2s2p^2P^e$  state is in a very good agreement with the results obtained from variational calculations on the real axis [17,18] even though these did not contain the continuum shift. The agreement of the present results with our previous ones [28], also obtained by the CCR method, is not accidental. In Ref. [28] we showed that the conver-

gence of the CCR computation of the  $2s2p^2P^e$  state was very good. In the present work we changed and enlarged the basis set a little. The results are essentially the same.

The positions of the  $2p^3D^o$  and  $2s2p^2P^e$  states obtained in present work are about 0.17 eV lower than those of Nicolaides, Piangos, and Komninos [27]. Their widths differ from the present ones by about 50 meV. As regards the relative position to the nearest threshold, this difference is without consequence for the  $2p^3D^o$  state.

TABLE II. Triply excited  $n=2$  intrashell resonances of  $\text{He}^-$ . The energy positions  $E$  (eV) with respect to the He ground state and the widths  $\Gamma$  (meV).

Threshold	Resonance	This work		Other theoretical results		Ref.	
		$E^a$	$\Gamma^a$	$E^a$	$\Gamma^a$		
$2p^2P^e$	59.64						
	$2s2p^2P^e$	59.537	32	59.70	79	[27]	
	$2p^3D^o$	59.288	331	59.45	282	[27]	
				59.5		[41]	
$2s2p^3P^o$	58.309						
	$2s2p^2D^e$	58.303	49		b		
$2s^2S^e$	57.84	$2s2p^2P^e$	57.412	10.3	57.413		[17]
					57.412		[18]
					57.412 <sup>c</sup>	10.4 <sup>c</sup>	[28]
					57.427 <sup>d</sup>	15 <sup>d</sup>	[28]
	$2s^2p^2P^o$	57.205	71		e		

<sup>a</sup>The energies have been converted from atomic units using the value of  $-2.903724$  a.u. as the ground-state energy of He, and  $1 \text{ a.u.} = 27.2079 \text{ eV}$ .

<sup>b</sup>For comparison with other theoretical and experimental results, see Table IV below.

<sup>c</sup>Computed by the CCR method.

<sup>d</sup>Obtained by a medium-size computation using the state-specific complex-energy approach.

<sup>e</sup>For comparison with other theoretical and experimental results, see Table III below.

Indeed, this resonance definitely lies between the  $2s2p^3P^o$  and  $2p^23P^e$  thresholds and its width is about 0.3 eV. As regards the  $2s2p^22P^e$  state, the lowering of its energy is what had been anticipated in Ref. [27] for a larger calculation of the localized correlation. Thus the  $\text{He}^- 2s2p^22P^e$  resonance is indeed about 0.1 eV below the  $2p^23P^e$  level. For the width of  $2s2p^22P^e$  we obtained  $\Gamma=32$  meV, which is more than twice as small than the value obtained by Nicolaides, Piangos, and Komninos [27]. This difference reflects the importance of the various interactions which were included in this work (see the Introduction), but were neglected in [27].

Our results for the energy and width of the  $2s^22p^2P^o$  resonance are  $E=57.205$  eV and  $\Gamma=71$  meV. In Table III they are compared with the literature data. The width disagrees with the value of 2.4 meV computed by Smith *et al.* [14]. On the other hand, it is in quite good agreement with the experimental value of 90 MeV obtained by Quéméner, Paquet, and Marmet [6] (the result given originally by the authors is corrected by a factor of 2 as in Ref. [8]) and by Marchand [8]. The position of the  $2s^22p^2P^o$  resonance agrees very well with the experimental data. Taking into account the experimental uncertainties, only the Quéméner, Paquet, and Marmet [6] experiment does not cover our result. Nevertheless, the discrepancy is quite small even in that case. The saddle-point and Feshbach-projection results [18] agree with the results of experiments and of this work. However, the calculations of [18] do not contain the continuum contribution, which could shift the energy either up or down.

The case of the  $2s2p^22D^e$  resonance has attracted considerable theoretical and experimental attention (see Table IV). It contains strong-correlation effects while at the same time it lies very close to the  $\text{He} 2s2p^3P^o$  autoionizing state at 58.31 eV. Therefore, the accurate determination of its position and its width requires the use of function spaces capable of representing the details

of the localized as well as the asymptotic correlation. For example, a recent reasonably large state-specific calculation of  $\Psi_0$ , the square-integrable part of the resonance [13,27] containing the localized correlation, put this resonance below the  $\text{He}^3P^o$  threshold [38]. However, since the continuum shift turned out to be positive [38], the resonance position was pushed just above the  $\text{He}^3P^o$  threshold. This indicated that an even larger calculation of both the localized and asymptotic correlations, such as the present one, ought to be carried out for the results to be definitive. The results of the present work,  $E=58.303$  eV and  $\Gamma=49$  meV, are in accordance with the accurate experimental results [6,11]. This implies that this resonance is real and of Feshbach type [13,26,27,25,17,39].

#### IV. SYNOPSIS

In order to compute reliably the positions and widths of negative-ion multiply excited resonances, the theoretical method must account for all the interactions contributing to the stability and localization as well as for the decay of the state into a multichannel (in general) continuum. The possibility of using square-integrable basis sets, real or complex, has the serious advantage that these interactions can be computed to all orders via diagonalization of appropriate matrices which produces complex eigenvalues [28,32]. In previous work [40] it was shown that the interaction of two free electrons in the continuum can be calculated using a Hamiltonian with real coordinates and an expansion over antisymmetrized products of complex functions. In the present work, the demand of high accuracy has led us to the execution of large calculations where the Hamiltonian has complex coordinates and the trial function is a superposition of correlated configurations [28,33–35] containing the effects of both the closed and the open channels. Up to 1300 terms

TABLE III. The energy  $E$  and the width  $\Gamma$  of the  $2s^22p^2P^o$  resonance.

Reference	Method	$E$ (eV)	$\Gamma$ (meV)
Experimental			
Kuyatt <i>et al.</i> [4]		57.1±0.1	
Grissom <i>et al.</i> [5]		57.21±0.06	
Quéméner <i>et al.</i> [6]		57.15±0.04	90±14
Sanche and Schulz [7]		57.16±0.05	
Marchand [8]		57.2±0.05	90±200
Hicks <i>et al.</i> [9]		57.22±0.04	
Roy <i>et al.</i> [10]		57.19±0.03	
Theoretical			
Eliezer and Pan [12]	Stabilization	57.3	
Nicolaides [13]	State specific	57.3	
Smith <i>et al.</i> [14]	Close coupling	56.48	2.4
Ahmed and Lipsky [15]	Truncated diagonalization	57.35	
Nesbet [16]	Stabilization	57.41	
Bylicki [18]	Feshbach projection	57.196 <sup>a</sup>	
Chung quoted in Ref. [18]	Saddle point	57.207 <sup>a</sup>	
This work	Complex-coordinate rotation	57.205 <sup>a</sup>	71

<sup>a</sup>The energies have been converted from atomic units using the value of  $-2.903724$  a.u. as the ground-state energy of He, and  $1$  a.u. =  $27.2079$  eV.

TABLE IV. The energy  $E$  and the width  $\Gamma$  of the  $2s2p^2D^e$  resonance.

Reference	Method	$E$ (eV)	$\Gamma$ (meV)
Experimental			
Kuyatt <i>et al.</i> [4]		58.2±0.1	
Grissom <i>et al.</i> [5]		58.31±0.08	
Quéméner <i>et al.</i> [6]		58.23±0.04	50±20
Sanche and Schulz [7]		58.25±0.05	
Marchand [8]		58.3±0.05	
Hicks <i>et al.</i> [9]		58.30±0.04	
Roy <i>et al.</i> [10]		58.29±0.03	
Gosselin and Marmet [11]		58.283±0.003	59±4
Theoretical			
Eliezer and Pan [12]	Stabilization	58.3	
Nicolaides [13]	State specific	58.4	
Smith <i>et al.</i> [14]	Close coupling	58.34	24.6
Nesbet [16]	Stabilization	58.52	
This work	Complex-coordinate rotation	58.303 <sup>a</sup>	49
Position of the $2s2p^3P^o$ threshold			
Gosselin and Marmet [11]	Scattering experiment	58.309±0.003	
Mannervik [42]	Spectroscopical experiment	58.312±0.003	
Ho [43]	Complex-coordinate rotation	58.313 <sup>a</sup>	

<sup>a</sup>The energy has been converted from atomic units using the value of  $-2.903\,724$  a.u. as the ground-state energy of He, and 1 a.u. = 27.2079 eV.

(for the  $\text{He}^- 2s2p^2D^e$  resonance) were included in the trial function so as to establish good convergence.

Reliable results were obtained for five  $\text{He}^-$  resonances:  $2s^22p^2P^o$ ,  $2s2p^2D^e$ ,  $2s2p^2^4P^e$ ,  $2s2p^2^2P^e$ , and  $2p^3D^o$ . For the  $2s^22p^2P^o$  and  $2s2p^2D^e$  states the computed parameters are in good agreement with the experimental data. In particular, the  $2s2p^2D^e$  position was obtained below the  $2s2p^3P^o$  threshold, settling the 15-year-old, ap-

parently open question [17,25–27,39]. The  $2s2p^2^4P^e$ ,  $2s2p^2^2P^e$ , and  $2p^3D^o$  resonances have not been observed. Their parameters obtained in this work should help possible future experiments. We did not obtain the intrinsic parameters of two other  $n=2$  intrashell  $\text{He}^-$  resonances, the  $2s2p^2S^e$  and the  $2p^3P^o$ , since the calculations did not produce sufficiently stable results. We will come back to this problem in the near future.

- [1] U. Fano and J. W. Cooper, *Phys. Rev.* **138**, A400 (1965).  
[2] D. R. Beck and C. A. Nicolaides, *Chem. Phys. Lett.* **59**, 525 (1978).  
[3] C. A. Nicolaides and Y. Komninos, *Chem. Phys. Lett.* **80**, 463 (1981).  
[4] C. E. Kuyatt, J. A. Simpson, and S. R. Mielczarek, *Phys. Rev.* **138**, A385 (1965).  
[5] J. T. Grissom, R. N. Compton, and W. R. Garrett, *Phys. Lett.* **30A**, 117 (1969).  
[6] J. J. Quéméner, C. Paquet, and P. Marmet, *Phys. Rev. A* **4**, 494 (1971).  
[7] L. Sanche and G. J. Schulz, *Phys. Rev. A* **5**, 1672 (1972).  
[8] P. Marchand, *Can. J. Phys.* **51**, 814 (1973).  
[9] P. J. Hicks, C. Cvejanović, J. Comer, F. H. Read, and J. M. Sharp, *Vacuum* **24**, 573 (1974).  
[10] D. Roy, A. Delâge, and J.-D. Carette, *J. Phys. B* **11**, 4059 (1978).  
[11] R. N. Gosselin and P. Marmet, *Phys. Rev. A* **41**, 1335 (1990).  
[12] I. Eliezer and Y. K. Pan, *Theor. Chim. Acta* **16**, 63 (1970).  
[13] C. A. Nicolaides, *Phys. Rev. A* **6**, 2078 (1972).  
[14] K. Smith, D. E. Golden, S. Ormonde, B. W. Torres, and A. R. Davis, *Phys. Rev. A* **8**, 3001 (1973).  
[15] A. Ahmed and L. Lipsky, *Phys. Rev. A* **12**, 1176 (1975).  
[16] R. K. Nesbet, *Phys. Rev. A* **14**, 1326 (1976).  
[17] K. T. Chung and B. F. Davis, in *Autoionization: Recent Developments and Applications*, edited by A. Temkin (Plenum, New York, 1985), p. 73.  
[18] M. Bylicki, *Phys. Rev. A* **45**, 2079 (1992).  
[19] D. Spence, *Phys. Rev. A* **12**, 2353 (1975).  
[20] P. J. M. van der Burgt, J. van Eck, and H. G. M. Heidemann, *J. Phys. B* **18**, L171 (1985).  
[21] S. Ormonde, F. Kets, and H. G. M. Heidemann, *Phys. Lett.* **50A**, 147 (1974).  
[22] C. A. Nicolaides and D. R. Beck, *J. Chem. Phys.* **66**, 1982 (1977).  
[23] E. Träbert, P. H. Heckmann, J. Doerfert, and J. Granzow, *J. Phys. B* **25**, L353 (1992).  
[24] K. T. Chung, *Phys. Rev. A* **20**, 724 (1979).  
[25] K. T. Chung, *Phys. Rev. A* **22**, 1341 (1980).  
[26] C. A. Nicolaides, *Phys. Rev. A* **46**, 690 (1992).  
[27] C. A. Nicolaides, N. A. Piangos, and Y. Komninos, *Phys. Rev. A* **48**, 3578 (1993).  
[28] M. Bylicki and C. A. Nicolaides, *Phys. Rev. A* **48**, 3589 (1993).  
[29] C. A. Nicolaides and S. I. Themelis, *J. Phys. B* **26**, L387 (1993).

- [30] B. Simon, *Ann. Math.* **97**, 247 (1973).
- [31] G. Doolen, *J. Phys. B* **8**, 525 (1975).
- [32] B. R. Junker, *Adv. At. Mol. Phys.* **18**, 207 (1982).
- [33] M. Bylicki, *J. Phys. B* **24**, 413 (1991).
- [34] W. Woźnicki, in *Theory of Atomic Shells in Atoms and Molecules*, edited by A. Jucys (Vilnius, Mintis, 1971), p. 103.
- [35] J. Muszyńska, D. Papierowska, and W. Woźnicki, *Chem. Phys. Lett.* **76**, 136 (1980).
- [36] H. M. James and A. S. Coolidge, *Phys. Rev.* **49**, 688 (1936).
- [37] C. A. Nicolaides, in *Advanced Theories and Computational Approaches to the Electronic Structure of Molecules*, edited by C. E. Dykstra (Reidel, Dordrecht, 1984), p. 161.
- [38] G. Aspromallis, Th. Mercouris, and C. A. Nicolaides (unpublished).
- [39] K. T. Chung, *Phys. Rev. A* **46**, 694 (1992).
- [40] Th. Mercouris and C. A. Nicolaides, *Phys. Rev. A* **48**, 628 (1993).
- [41] M. Bylicki (unpublished).
- [42] S. Mannervik, *Phys. Scr.* **40**, 28 (1989).
- [43] Y. K. Ho, *Phys. Rev. A* **48**, 3598 (1993).